J Food Sci Technol (March 2023) 60(3):1153–1162
https://doi.org/10.1007/s13197-023-05669-4

ORIGINAL ARTICLE

Development and characterization of novel packaging films from composite mixtures of rice-starch, tara gum and pectin

Marcia Quequezana Bedregal[1] · **Elizabeth Medrano de Jara**[1] · **Humberto Palza Cordero**[2] · **Luis Miranda Zanardi**[1]

Revised: 29 November 2022 / Accepted: 16 January 2023 / Published online: 28 January 2023

Abstract Biodegradable films intend to replace polymers derived from petroleum. The effect of pectin and Tara gum on the properties of films prepared with rice starch and glycerol was studied in this context. FTIR analysis determined the presence of complex interactions between the components. SEM showed regular film surface with minor roughness. The evaluation of mechanical properties of the films proved the importance of pectin, Tara gum and glycerol concentration. When the proportion of pectin to Tara gum was 1:1, the tension at break, the elongation and the solubility reached the highest values while the water vapor permeability dropped to a minimum. Statistical analysis demonstrated non-linear behavior between composition and properties of the films and stated the importance of interactions between the components. Films produced from rice starch and glycerol in combination with pectin and Tara gum present competitive properties in terms of elongation, tensile stress, permeability to water vapor and solubility, displaying a uniform structure suitable for the packaging of food materials.

✉ Luis Miranda Zanardi
lmirandaz@unsa.edu.pe

Marcia Quequezana Bedregal
mquequezanab@unsa.edu.pe

Elizabeth Medrano de Jara
emedrano@unsa.edu.pe

Humberto Palza Cordero
hpalza@ing.uchile.cl

[1] Department of Chemical Engineering, Universidad Nacional de San Agustin de Arequipa, Santa Catalina 117, Cercado, Arequipa 04001, Perú

[2] Department of Chemical Engineering, Biotechnology and Materials, School of Physical and Mathematical Sciences, University of Chile, Beauchef 851, Santiago, Chile

Keywords Rice starch · Film properties · Glycerol · Tara gum · Pectin

Abbreviations

GLY	Glycerol
PEC	Pectin
RST	Rice starch
TAG	Tara gum

Introduction

The large volume of accumulated non-degradable plastic material creates an environmental problem, affecting life on our planet. Therefore, various agro-industrial residues have been tested as possible sources of low-cost, biodegradable plastics (Ferreira et al. 2016a, b). Rice is a low-cost source of starch, protein and minerals. Rice starch (RST) can be produced from broken rice generated in the milling process. This may be used as raw material in the manufacture of biodegradable films and coatings. Starch is mainly made up of two components: amylose, linear in nature, and amylopectin, which has branches. The highly hydrophilic character of starches negatively affects the mechanical and barrier properties of films destined for packing applications (Ferreira et al. 2016a, b). The properties of films are determined by their composition, the structure of the starch granules and the manufacturing process. The behavior of starch-based films may be improved by adding plasticizers such as glycerol (GLY). GLY increases the thickness and elongation of films but reduces their tensile stress (Sapper and Chiralt 2018). The use of gums or hydrocolloids also modifies the properties of starch films. Pectin (PEC) is a bio-based compound that improves the properties of starch, it is a polysaccharide

mixture with a complex structure of at least 65% galacturonic acid (Ga) Hydroxyl groups of galacturonic acid, amides and carboxyls strongly interact with water by connecting macromolecules. The interaction between PEC and water can be affected by the monovalent cations of PEC, as well as its amorphous character, particle size, surface area and porosity. PEC can inhibit the dehydration of starch gels due to its high water holding capacity (Zhai et al. 2021).

Tara gum (TAG) is a neutral polysaccharide obtained from the seed endosperm of the *Caesalpinia Spinosa* tree. It has a galactomannan nature with a 3:1 ratio of mannose to galactose (Lee et al. 2017). TAG is polydisperse with high molecular weight, between 1 and 2.5 million Daltons. Lee et al. (2017) report that TAG reduced the high thixotropy of RST.

The properties of starch films could be further improved by combining different bio-based compounds. For biofilm design it is necessary to consider the compatibility of the components involved, like RST, PEC and TAG, as well as the synergy effects that may occur between them. The compatibility of biopolymers defines if the properties of binary blends are advantageous. Miscibility describes the behavior of a polymer pair by specifying the number of phases and their composition formed upon blending. All polymers are partially miscible and dissolve in each other to some extent, and mutual solubility depends on interactions (Imre and Pukánszky 2013). The combination of a thickening hydrocolloid, like TAG, with a gelling hydrocolloid, such as PEC, may provide benefits as a result of their interaction (Nautiyal 2012).

Few works address the interaction of hydrocolloids among themselves and with plasticizers, and their influence on the properties of films. Specifically, the effect of a mixture of PEC and TAG on the properties of RST has not been previously addressed. Therefore, this work evaluates the individual and combined effect of PEC and TAG on the properties of biodegradable films made from RST. The findings of this work may offer significant steps forward regarding the use of hydrocolloid mixtures in the formulation of packaging films. An explanation is also offered concerning the interaction of participating components.

Materials and methods

Materials

Analytical grade GLY, PEC, sodium hydroxide, hydrochloric acid (Sigma-Aldrich) and silica gel with moisture indicator (Merck KGaA) were used. TAG was purchased from Somerex (Peru).

Rice starch extraction

Starch was obtained from the Tacuari rice variety grown in Arequipa, Peru, applying alkaline extraction with 0.05 M NaOH, and using the method reported by Devi et al. (2009). The rice grains were wet milled in an Osterizer blender, the content was collected, sedimented and decanted. The settled starch was re-suspended in 0.05 M NaOH solution with a mechanical stirrer at 200 RPM and room temperature. The solution was allowed to stand for 8 h, and the supernatant was discarded, followed by washing with distilled water and neutralization with 1 M HCl, and then dehydrated at 40 °C for 24 h using a tray dryer with recirculating air. The starch obtained was pulverized and classified by size in a WS Tyler brand Ro-Tap® model RX-29, selecting the particles smaller than 150 µm (Tyler mesh No. 100).

Compositional analysis of rice starch

The following methods have been applied to characterized rice starch: humidity: NTP 209.067:1974; ashes: AOAC 2.173; fat: NTP 209.093 (ISO 3961:2017); protein (X 6.25): AOAC 2.057; fiber: NTP 209.074 (NTP 2018); carbohydrates: AOAC 31.043 (Latimer 2016).

Amylose and amylopectin ratio was determined using the Megazyme enzyme kit (Sigma Aldrich) by a colorimetric method measuring the absorbance at 510 nm. Amylopectin was precipitated with concanavalin A, leaving amylose in the supernatant, which was hydrolyzed to glucose.

Preparation film process

The film-forming solutions were prepared with 2.5 g of RST and the amounts of TAG, PEC, GLY and distilled water according to the experimental mixture design. The solutions were stirred at 700 RPM and 70 °C for 30 min, then, the temperature was increased to 92 °C for 10 min. For bubble removal, the solution was placed in a Martin Walter/Powersonic 230D ultrasonic bath for 5 min at 50 °C and 5 pulses. The film-forming solutions were cast into glass molds. Drying of the film solution was carried out in a Memmert UF 260 Plus oven at 40 ºC for 16 h, with 70% opening and 30% air circulation. Afterwards, the films were removed from the molds and stored in hermetically sealed plastic bags.

Evaluation of barrier and mechanical properties

The thicknesses of the films were evaluated with a Mitutoyo Digimatic micrometer, model MDC-01 MJ

(+ 0.001 mm). Each sample was measured in five different areas, using the average thickness for tension at break, elongation at break and water vapor permeability.

The measurement of the tension and elongation at break followed the ASTM D 882–02 standard, using a Mecmesin Multitest 0.5-i model dynamometer, equipped with Software Emperor Force v1.18. The film sample was cut into 10 × 2 cm size strips. All film strips were equilibrated at 50% RH (± 5%) for 48 h at room temperature.

The water vapor permeability of the films was determined using the ASTM E 96–80 standard. A circular section of 0.7 mm diameter was cut from each film, measuring its thickness and placing the sample on top of a 2 ml vial, containing 1 ml of supersaturated potassium nitrate (KNO_3) solution. To generate constant relative humidity, the vials were placed in a desiccator containing silica gel as a drying agent. The test was performed in triplicate and the variation in weight of the vial was recorded every hour on an analytical balance with a precision of 0.0001 g for 8 continuous hours.

The solubility of the films was determined applying the ASTM D570-98 standard. Samples of 2 × 2 cm were weighed and placed in vials with 30 ml of distilled water for 24 h at room temperature. The undissolved samples were dried at 100 °C in an oven for 24 h and weighed again to obtain the final dry weight.

Film chemical bonding characterization or FTIR analysis

Evaluation of the chemical nature of the participating components and the resulting films was performed by infrared spectroscopy with inverse Fourier transform (FTIR). Spectra were recorded at room temperature using a Perkin Elmer Spectrum Two FTIR spectrophotometer in the range of 400 to 4000 cm^{-1} showing a 0.5 cm^{-1} resolution. The instrument was controlled by Spectrum® v 10.5.4 software, and used an Attenuated Total Reflectance (ATR) accessory that features a single bounce ZnSe–diamond crystal. For each sample, four scans were performed.

Microstructural analysis

The morphology of the rice starch surface and the cross-sectional microstructure of the films were determined by scanning electron microscopy (SEM) in a ZEISS Model EVO| MA10 with magnifications of 500 and 1500×, voltage of 15 kv, WD 9.5. The software used was SEMZEISS. The films were held on a double-glue support and sputter coated with gold-platinum to work in high vacuum mode.

Experimental design and data processing

The experiments were organized in stages. The first stage considered a basic formulation of RST and GLY to determine the concentration range for both components. The second stage included TAG and PEC in the formulas. A mixture design of extreme vertices with centroid and axial points of third degree, with 27 experiments, that were triplicated was applied (Machado et al. 2019). The mass of RST was held constant at 2.5 g, and the sum of the masses of TAG and PEC was 0.5 g or lower. Thus, the masses of both gums varied between 0.1 g and 0.4 g. GLY was used in the range of 1.26 g and 1.89 g. For each sample the total mass of 100 g was completed with distilled water. In the mixture design the levels considered for TAG and PEC were 0.10, 0.15, 0.20, 0.25, 0.30, 0.40 g, while the levels for glycerol were 1.260, 1.4175, 1.575, 1.7325, 1.890.

The third experimental stage selected the most promising samples and add the evaluation of solubility and water vapor permeability tests. Based on the experimental results and the mathematical models derived from them, interaction among the components was estimated and local optima were searched.

Because all the experiments were triplicated, the results were represented by their standard mean values. Statistical analysis has been performed to the experimental results with a 95% confidence level. The Analysis of Variance (ANOVA) was used to showcase the significance of each component and the interactions between them. The Tukey test determines the significance of each component and their interactions on the properties of the films.

The films were coded as A1, A2, … A27. Table 2 shows the composition of each sample.

Results and discussion

Composition of rice starch

Patindol et al. (2007) indicated that the amylose/amylopectin ratio of starch from large grain rice varied between 17.0 and 35.7%. The amylose/amylopectin percentage reported in Table 1 is close to the lower limit, meaning that the amylopectin concentration is high.

The textural properties of starch also depend on the molecular size of amylose and the length of amylopectin chains. Smaller molecular sizes for both amylose and amylopectin correspond to rice varieties with higher amylose content (Li et al. 2018). Therefore, for the Tacuari RST relatively high molecular sizes are expected.

Table 1 Composition of rice starch

Compound	Unit	Result
Humidity	% (w/w)	7.46
Ash	% (w/w)	0.33
Fat	% (w/w)	1.07
Proteins (X 6.25)	% (w/w)	0.71
Fiber	% (w/w)	3.14
Carbohydrates	% (w/w)	80.91
Energy	kcal/100 g	367.6
Amylose/Amylopectin	% (w/w)	17.44

FTIR spectra

Figure 1 shows the FTIR spectra from broken RST, PEC, TAG, GLY as well as a representative film, sample A14 in Table 2 (composition in mass %: 58.7, RST; 29.6, GLY; 5.9, TAG; and 5.9, PEC). A first inspection of Fig. 1 shows that the spectrum of sample A14 is influenced by the participant components in the following order: GLY, RST, TAG and PEC. Also, higher absorbances are located at the neighborhood of the following wavenumbers: 3300, 2900, 1650, 1400 and 1000 cm^{-1}.

Molecular interaction is mainly expressed through hydrogen bonds. The 3400—3200 cm^{-1} bandwidth corresponds to polyhydroxyl groups (Khatun et al. 2021), representing the vibrations of the intramolecular -OH groups of the absorbed water, GLY and RST as well as the participating gums. The peak located at 2926 cm^{-1} is associated with the vibration of hydrogen bonds and appears sharp in the spectra of GLY, RST, TAG and the resulting film.

The polysaccharides—RST, TAG and PEC—show a common peak at about 1643 cm^{-1} corresponding to the −OH bending of the water, indicating its hygroscopic nature (Ferreira-Villadiego et al. 2018). In fact, bands between 1620 and 1412 cm^{-1} are attributed to the absorbance of the different water-soluble polysaccharides, as well as bands close to 1400 cm^{-1} that correspond to the stretching of the group (C = O); while the absorption bands between 1200 and 800 cm^{-1} are characteristic of carbohydrates (Shehata et al. 2020).

The region of the saccharides is limited by the bands between 1165 and 980 cm^{-1}. The length of the band located at 1000 cm^{-1} was related to the fraction of amorphous structures, mainly RST, TAG and film A14, and may indicate that water acted intermolecularly through hydrogen bonds. This region presents higher absorbance values for all the participant components. The spectrum of pure GLY showed five typical absorption bands between 800 and 1150 cm^{-1}, corresponding to the vibrations of C–C and C–O.

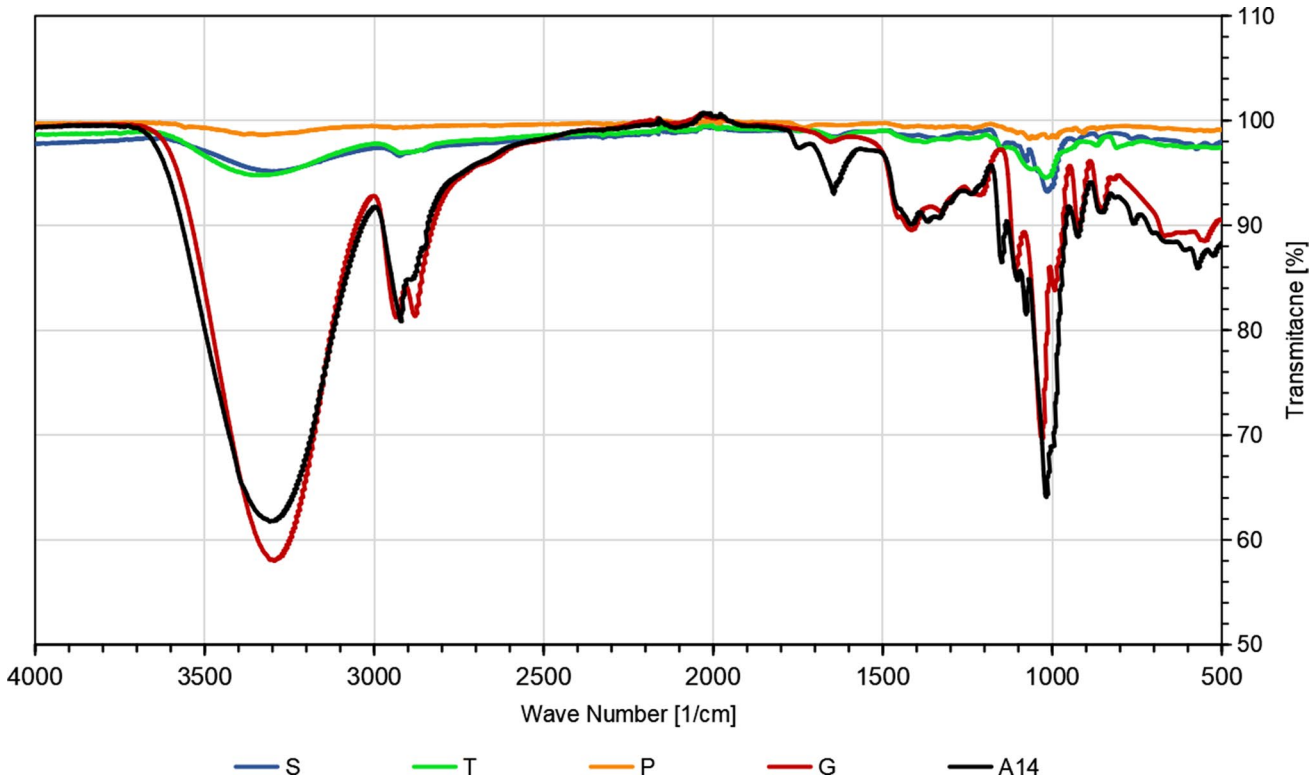

Fig. 1 FTIR spectra of components and selected film

Table 2 Mechanical properties of films obtained by mixture design

Code	Tara g	Pectin g	Glycerol g	Thickness mm	Elongation %	Tension MPa
A01	0.10	0.10	1.2600	0.113	53.91	2.040
A02	0.10	0.10	1.5750	0.127	65.78	1.656
A03	0.10	0.10	1.8900	0	0.00	0.000
A04	0.10	0.25	1.2600	0.12	48.15	3.803
A05	0.10	0.25	1.5750	0.132	64.52	2.261
A06	0.10	0.25	1.8900	0.142	65.83	1.546
A07	0.10	0.40	1.2600	0.128	40.74	5.454
A08	0.10	0.40	1.5750	0.134	60.79	3.011
A09	0.10	0.40	1.8900	0.144	61.00	2.127
A10	0.15	0.15	1.4175	0.132	64.06	2.599
A11	0.15	0.15	1.7325	0.137	69.24	1.675
A12	0.15	0.30	1.4175	0.132	60.29	3.276
A13	0.15	0.30	1.7325	0.136	59.72	2.246
A14	0.20	0.20	1.2600	0.124	46.28	4.504
A15	0.20	0.20	1.5750	0.137	64.51	2.730
A16	0.20	0.20	1.8900	0.143	69.48	1.762
A17	0.25	0.10	1.2600	0.122	53.81	3.930
A18	0.25	0.10	1.5750	0.131	59.53	2.521
A19	0.25	0.10	1.8900	0.152	67.37	1.301
A20	0.25	0.25	1.2600	0.118	49.32	5.512
A21	0.25	0.25	1.5750	0.145	62.85	2.698
A22	0.25	0.25	1.8900	0.159	69.18	2.280
A23	0.30	0.15	1.4175	0.134	60.66	3.567
A24	0.30	0.15	1.7325	0.139	67.43	2.078
A25	0.40	0.10	1.2600	0.13	52.90	4.310
A26	0.40	0.10	1.5750	0.14	59.24	3.109
A27	0.40	0.10	1.8900	0.146	71.34	2.079

The interaction present between water, GLY, RST and gums can be inferred from the comparison of the spectra of the pure components and their shift in the spectrum of the resulting film. As can be seen the spectrum of film A14, this is not just a sum of the participating components spectra, this fact is more noticeable at 1626 and 1078–1000 cm^{-1}. GLY presents a peak at 1654 cm^{-1} and the film shifts to 1626 cm^{-1}, corresponding to -OH bending related to the hygroscopic nature of the film. The film peak at 1019 cm^{-1}, located in the region of the saccharides, presents a shift from the 1031 cm^{-1} GLY peak. Such displacements indicate the interaction between the components of the film.

By comparing the spectra of several films (results not shown), it is observed that the effect of the Tara gum/pectin ratio on the FTIR spectra is small, becoming more pronounced in the following wavenumbers: 2920; 1413; 1100 and 1000 cm^{-1}. In addition, the effect of glycerol concentration in the spectra was detected along the same wavenumbers.

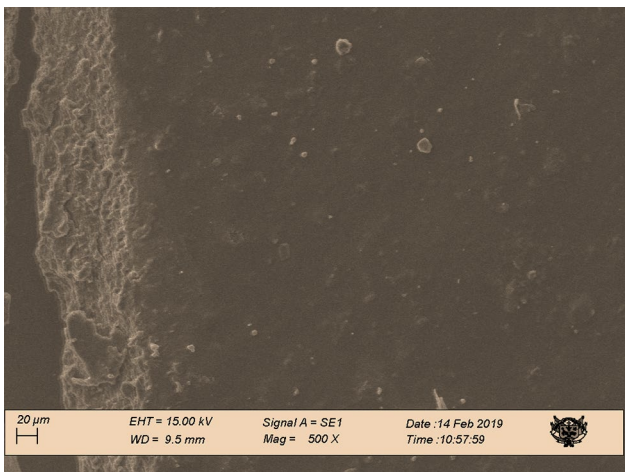

Fig. 2 Scanning electron microscope (SEM) photographs of film composed by 0.40 g TAG, 0.10 g PEC, 1.26 g GLY and 2.5 g of RST

Microscopy of starch and selected sample

Figure 2 shows a scanning electron microscope (SEM) representative image with a magnification of 1580 of the side section of the film containing 0.40 g of TAG, 0.1 g of PEC and 1.26 g of GLY, sample A25 in Table 2. Some minor roughness was observed, the surface was regular without cracks not compromising the properties of the films. The cross-sectional area shows the film's spongy structure. Accordingly, RST films blended with carboxymethyl cellulose exhibited an homogeneous cross-sectional surface (Suriyatem et al. 2019). SEM views of RST granules (not shown), display angular, polyhedral shapes, of a size between 6 to 8 microns (μm). The size, shape and structure of the starch granules differ due to their botanical origin, with RST corresponding to a polyhedral form between 2 to 5 microns in size (Wang et al. 2010).

Film thickness and mechanical properties

The mass of the non-water components of the film samples prepared ranged from 3.96 to 4.99 g, and the thicknesses varied from 0.113 to 0.159 mm. Table 2 presents the results of mechanical properties. Table 2 shows that formula A03 did not get to form a firm structure.

There is a linear relationship between the thickness of the films and their mass. In order to examine the contribution of GLY, PEC and TAG to the thickness of the films, Fig. 3 presents three data series corresponding to films with different mass of GLY: 1.26 g (black); 1.575 g (dotted); and 1.89 g (grey). As can be observed, the concentration of plasticizer directly increases the thickness of the films.

Aghazadeh et al. (2018) explained that when incorporating a plasticizer in a starch matrix, the intramolecular affinity between the starch chains decreases due to the formation of hydrogen bonds between the plasticizer molecules and the starch. Therefore, the matrix of the film occupies a greater volume, obviously increasing the film thickness and facilitating the movement of starch chains, giving the films greater flexibility.

The effect of the mass fraction of TAG over the summation of the masses of TAG and PEC $[T/(T+P)]$ on the film thickness is represented in Fig. 3a. The content of Tara gum did not show a linear relation to film thickness, which indicated interaction between the participating components, mainly TAG and PEC.

Therefore, the ANOVA reveals that the concentration of GLY, TAG and PEC, as well as their triple interaction, present a statistically significant effect on the thickness of the films. Tukey's test shows that GLY concentration offers a statistical difference in terms of the thickness of the films, but the percentage of TAG (100 T/(T + P)) does not have a significant effect.

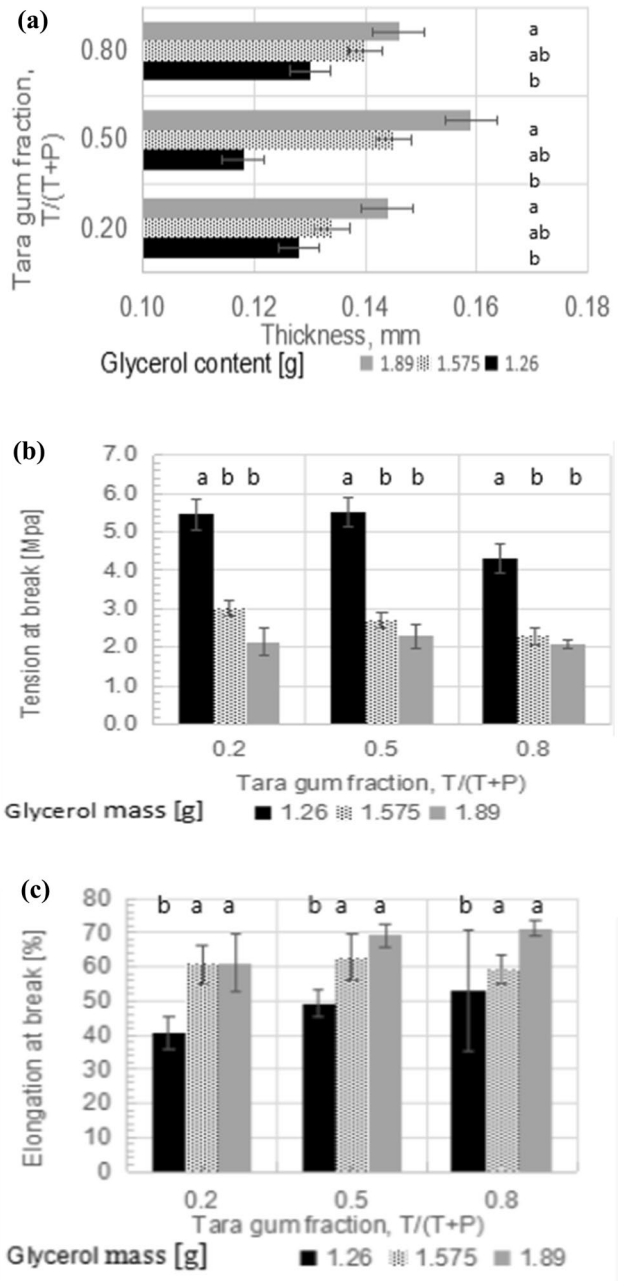

Fig. 3 Thickness and mechanical properties of films: Thickness **b** Tension at break; **c** Elongation at break. *T* and *P* are the masses of Tara gum and pectin in grams

The tension at break and the elongation at break are the most relevant mechanical properties, presented in Fig. 3b and c, for three series with different content of glycerol; 1.26 g, 1.575 g and 1.89 g, respectively. As in Fig. 3a, the sum of masses of TAG and PEC was equal to 0.5 g, which implies that the proportions of TAG and PEC are complementary. For example, when the mixture contains 0.1 g of PEC, it should have 0.4 g of TAG, and vice versa.

The experimental tension values showed a wide range of variation. The data represented in Fig. 3b ranged from 2.08 to 5.51 MPa. It is clearly observed that the samples with the highest tension correspond to those containing the least amount of glycerol. When the mass of GLY is low (1.26 g), increasing TAG (reducing PEC) also reduces tension. However, increasing the GLY content does not reveal a noticeable or regular incidence, indicating complex interaction effects between the components. The following empirical equation was obtained from the experimental results of the mixture design:

$$F = a_1 T + a_2 P - a_3 G + a_4 W + a_{12} T * P + a_{13} T * G - a_{23} P * G - a_{123} T * P * G \quad (1)$$

Being: $a_1 = 5.279$; $a_2 = 11.074$; $a_3 = 2.620$; $a_4 = 0.044$; $a_{12} = 47.34$; $a_{13} = 0.418$; $a_{23} = 2.782$; $a_{123} = 28.497$.

Where G, P, T and W are the masses in grams of glycerol, pectin, Tara gum and water, respectively. The tension at break F is expressed in MPa.

The model terms containing GLY were more influential (reducing the tension value) as well as the interaction between TAG and PEC.

By applying Eq. (1) within the established composition ranges, it was found that the formula with the following mass percentages constitutes a local optimum for tension at break: RST, 58.7; GLY, 29.6; PEC, 7.0; and TAG, 4.7. In the present formulation, the participation of TAG, in addition to PEC and GLY when interacting with starch, generated a complex system of multiple interactions.

The elongation at break changed between 40.74 and 71.34 percent of the initial length of the films. Figure 3c presents some elongation results corresponding to three series of data with different GLY mass (1.26 g; 1.575 g and 1.89 g), showing that a higher plasticizer content increases the elongation. On the abscissa, the fraction of TAG is presented in reference to the sum of TAG and PEC. It is observed that when the concentration of TAG and PEC are equal, the elongation reaches higher values.

From the results, it is inferred that raising the GLY content reduces stress and increases the elongation. For corn, wheat, rice and potato starch films, maximum tensile strength varied from 4.48 to 8.14 MPa and elongation at break from 35.41 to 100.34% (Domene-López et al. 2019).

At low concentrations of GLY, TAG reduces stress and increases elongation. For a more detailed examination of the effect of TAG and PEC, new mechanical tests were carried out keeping the GLY content constant and equal to 1.26 g. The tension values obtained were in the range from 4.25 to 5.62 MPa; however, the elongation changed from 28.19 to 53.04%. It is noteworthy that the elongation profile showed a pronounced minimum corresponding to the composition of 40% TAG. Conversely, an almost linear decay was observed in the tension values when the content of TAG was higher.

The ANOVA applied to the experimental results of tension at break of the films finds that GLY, TAG and PEC, as well as the interaction between PEC and GLY, are statistically significant. Tukey's test determines that the concentration of GLY is statistically significant, while the percentage of TAG does not have a determining role.

For the elongation at break of the films, the ANOVA shows that only GLY and PEC are statistically significant. Tukey's test indicates that GLY concentration has a statistically significant effect, but the percentage of TAG (100 T/(T + P)) does not show an appreciable influence.

Water vapor permeability and solubility

The profile of water vapor permeability and solubility in terms of TAG content is presented in Fig. 4. The permeability values varied from 4.25 to 5.62 10^{-10} g s^{-1} m^{-1} Pa^{-1} for films containing 1.26 g of GLY and 2.50 g of RST.

A lower value can be observed when the amount of TAG and PEC are equal, corresponding to T/(T + P) = 0.5,

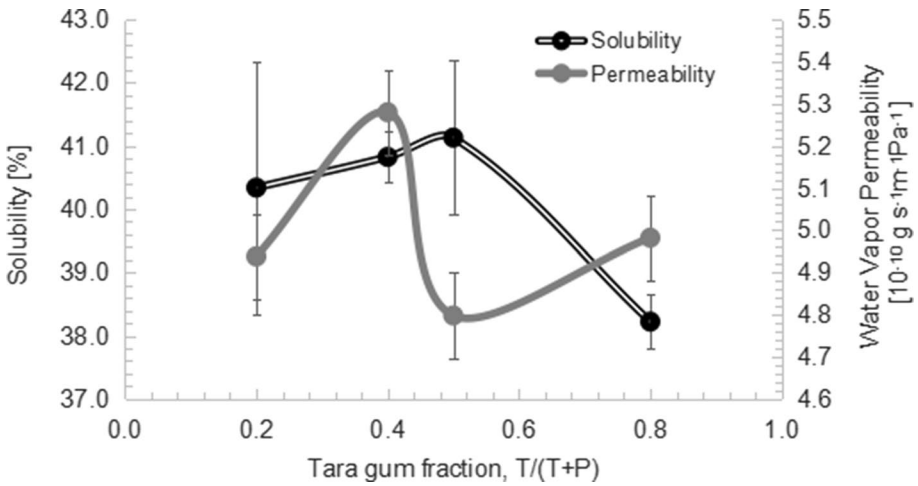

Fig. 4 Results of Water Vapor Permeability and Solubility. *T* and *P* are the masses of Tara gum and pectin in grams

convenient for packing purposes. The permeability of the films is influenced by several factors, such as the hydrophobicity or hydrophilicity of the participating components, the presence of cracks or breaks in the film as well as the tortuosity of the internal channels. Thakur et al. (2017) report a permeability value of 5.27 10^{-10} g s^{-1} m^{-1} Pa^{-1} for pea starch, chitosan and glycerol films, which is in agreement with our results.

The water solubility values, expressed as total mass percentage, are also presented in Fig. 4. The proportion of TAG and PEC in the films only slightly affected the water solubility values changing from 38.22 to 41.62%. In other words, when the content of GLYl is 1.26 g, equivalent to 29.6 mass percent of solids in the formula, and the amount of TAG and PEC are equal to 0.25 g, 5.9 mass percent, the lower value of water vapor permeability 4.25 10^{-10} g s^{-1} m^{-1} Pa^{-1} is obtained as well as a high value of elongation at break of 49.2% and a relative high value of tension at break equal to 5.42 MPa. Basiak et al. (2017) reported a solubility in water of 30.16% for wheat starch films with 33% GLY; the result of the present investigation is higher in this regard, equivalent to 41%.

The results mentioned add to the discussion of the relevance of different bio-based components on the characteristics of starch/glycerol films. The properties of blended starch–non starchy polysaccharide hydrocolloid systems depend on the structural characteristics of the components, the electrostatic interactions of starch with hydrocolloids, the ratio of hydrocolloids and the temperature of blend preparation as well as the cooling process (Saberi et al. 2017). Polysaccharides with high molecular weights, such as PEC and TAG, tend to develop intermolecular associations. The compatibility of RST depends on PEC's degree of esterification, high methoxyl PEC being more compatible. Likewise, the compatibility of RST with galactomannans depends on the mannose/galactose ratio (Li and Chien 2001). FTIR analysis established that the spectra of our resulting films were clearly influenced by RST, GLY, and TAG, with PEC occupying a weaker role. The importance of hydrogen bonds, hygroscopic behavior, and the presence of amorphous zones of the films are highlighted by such spectra. Satyamaiah et al. (2014) also report the formation of strong hydrogen bonds between Guar gum and PEC.

The film thickness, the tension at break, the elongation essays and the correspondent models demonstrated the complex incidence of GLY and TAG-PEC interaction. Yue Chen et al. (2020) also stated the synergy between TAG and PEC on films. It is noteworthy that the permeability to water vapor in our films, as well as their solubility, were only slightly reduced by increasing the concentration of TAG.

The interaction of RST with hydrocolloids, like TAG and PEC, is explained by amylose's binding affinity towards amylopectin chains and to other available hydrocolloids (Thakur et al. 2019). In the tapioca starch–TAG system, a phase separation process occurs due to thermodynamic incompatibility, in which TAG is located in the continuous phase and the starch granules increased in the disperse phase (Von Borries-Medrano et al. 2019). Lee et al. (2017), by confocal laser scanning microscopy, demonstrated a phase separation between RST and TAG, where TAG molecules separate into local domains. Also, this author found a synergistic effect on the rheological properties of TAG and RST blends.

In short, the participation of TAG, in addition to PEC and GLY, mixed in an aqueous RST solution, generated competing interactions among components, showing that composition and properties of the films are described by non-linear models. It is known that GLY expands the starch matrix due to hydrogen bonds (Basiak et al. 2018); that the PEC structure is modified by GLY (Costanza et al. 2019), and that TAG influences the properties of starch through a strong interaction with amylose (Lee et al. 2017).

Conclusions

Films obtained from RST and GLY in combination with PEC and TAG showed competitive properties in terms of elongation, tensile stress, permeability to water vapor and solubility, making up a uniform structure. RST, GLY, PEC and TAG in the presence of water make up a partially compatible compound.

TAG and PEC modified the properties of RST films even though their concentrations were below 12% of dry solids. The statistical analysis showed that RST establishes interactions with macromolecules of PEC and TAG as well as with GLY. PEC also promotes film dissolution. In contrast, TAG may constitute a continuous phase with PEC, causing the starch granules to increase their concentration in the dispersed phase.

A promising formulation for the films includes 29.6 mass percent of GLY and 5.9 mass percent of TAG as well as PEC. When the concentration of both hydrocolloids is equal their interaction shows higher values.

It is recommended to evaluate higher values of PEC and TAG concentrations in the film formulas to determine the trends of interaction between these components, and their impact on film properties.

Acknowledgements The financial support of Universidad Nacional de San Agustin de Arequipa, under contract IBA-023-2017-UNSA is deeply appreciated. We thank Esperanza Medina for providing the facilities of the Unit Operations research laboratory to conduct the experiments. We would also like to express our gratitude to Helbert Portugal, Christian Apaza and Brigitte Ortiz for their assistance along the experimental stage.

Authors' contributions LM, MQ and EM contributed to the study conception and design. Experimental work was performed by MQ and EM. Funding was managed by LM. Draft of the manuscript was written by LM. HP review and edit the document several times. All authors read and approved the final manuscript.

Funding The research leading to these results received funding from Universidad Nacional de San Agustin de Arequipa under Grant Agreement No. IBA-023–2017-UNSA.

Data availability The data that support the findings of this study are available on request from the corresponding author [LMZ]. The data are not publicly available due to the filing of a patent application that is part of the same research project.

Code availability Not applicable.

Declarations

Conflicts of interest The authors have no financial or proprietary interests in any material discussed in this article.

Ethics approval The authors declare that this research paper is original and has only been submitted to the Journal of Food Science and Technology. Our results are presented in an honest way without fabrication and we have acknowledged properly other works. If requested we are willing to send relevant documentation in order to verify the validity of the results presented.

References

Aghazadeh M, Karim R, Rahman RA, Sultan MT, Jhonson SK, Paykary M (2018) Effect of glycerol on the physicochemical properties of cereal starch films. Czech J. Food Sci. 36(5):403–409. https://doi.org/10.17221/41/2017-CJFS

Basiak E, Lenart A, Debeaufort F (2017) Effect of starch type on the physico-chemical properties of edible films. Int J Biol Macromol 98:348–356. https://doi.org/10.1016/j.ijbiomac.2017.01.122

Basiak E, Lenart A, Debeaufort F (2018) How glycerol and water contents affect the structural and functional properties of starch-based edible films. Polymers 10(4):412. https://doi.org/10.3390/polym10040412

Chen Y, Leilei X, Wang Y, Chen Z, Zhang M, Chen H (2020) Characterization and functional properties of a pectin/tara gum based edible film with ellagitannins from the unripe fruits of Rubus chingii Hu. Food Chem. https://doi.org/10.1016/j.foodchem.2020.126964

Costanza V, Bonanomi L, Moscato G, Wang L, Choi Y, Daraio C (2019) Effect of glycerol on the mechanical and temperature-sensing properties of pectin films. Appl Phys Lett. https://doi.org/10.1063/1.5121710

Devi A, Fibrianto K, Torley P, Bhandari B (2009) Physical properties of cryomilled rice starch. J Cereal Sci 49(2):278–284. https://doi.org/10.1016/j.jcs.2008.11.005

Domene-López D, García-Quesada JC, Martin-Gullon I, Montalbán MG (2019) Influence of starch composition and molecular weight on physicochemical properties of biodegradable films. Polymers 11(7):1084. https://doi.org/10.3390/polym11071084

Ferreira A, Alves V, Coelhoso I (2016a) Polysaccharides-based membranes in food packaging applications. Membranes 6:22. https://doi.org/10.3390/membranes6020022

Ferreira M, Linhares R, Martelli M (2016). In: Montero García M, Gómez-Guillén M, López Caballero M, Barbosa-Cánovas G (eds) Edible films and coatings: fundamentals and applications. CRC Press, Boca Raton. https://doi.org/10.1201/9781315373713

Ferreira-Villadiego J, García-Echeverri J, Vidal M, Pasqualino J, Meza-Castellar P, Lambis-Miranda H (2018) Chemical modification and characterization of starch derived from plantain (*Musa paradisiaca*) peel waste, as a source of biodegradable material. Chem Eng Trans 65:763–768. https://doi.org/10.3303/CET1865128

Imre B, Pukánszky B (2013) Feature Article: Compatibilization in bio-based and biodegradable polymer blends. Eur Polymer J 49:1215–1233. https://doi.org/10.1016/eurpolymj.2013.01.019

Khatun MA, Razzak M, Hossain MA, Rahman MA, Khan RA, Huque R (2021) Gamma radiation application to rice: Reduced glycemic index in relation to modified carbohydrate observed in FTIR spectra. Current Res Food Sci 4:11–17

Lee HY, Jo W, Yoo B (2017) Rheological and microstructural characteristics of rice starch–Tara gum mixtures. Int J Food Prop 20(S2):S1879–S1889. https://doi.org/10.1080/10942912.2017.1354884

Li TY, Chien JT (2001) Evaluation of rice starch-hydrocolloid compatibility at low-moisture content by glass transitions. J Food Sci 66(5):698–704

Li H, Wen Y, Wang J, Sun B (2018) Relations between chain-length distribution, molecular size, and amylose content of rice starches. Int J Biol Macromol 120(Pt B):2017–2025. https://doi.org/10.1016/j.ijbiomac.2018.09.204

Machado CM, Benelli P, Tessaro IC (2019) Constrained mixture design to optimize formulation and performance of foams based on cassava starch and peanut skin. J Polym Environ 27:2224–2238. https://doi.org/10.1007/s10924-019-01518-8

Nautiyal OH (2012) Effect of galactomannans and low esterified pectin combinations on fruit preparation syneresis, rheology and stability on storage. Int J Food Sci Nutrition Eng 2(2):6–11. https://doi.org/10.5923/j.food.20120202.02

NTP Norma Técnica Peruana (2018) NTP 209.066:1974- NTP 209.082:1974 referred to Starch properties evaluation. Resolucion Directoral N° 015-2018-INACAL/DN

Latimer G (2016) Official methods of analysis of AOAC International, 20th edn. AOAC International, Rockville (ISBN: 0935584870)

Patindol J, Gonzalez B, Wang YJ, McClung AM (2007) Starch fine structure and physicochemical properties of specialty rice for canning. J Cereal Sci 45:209–218. https://doi.org/10.1016/j.jcs.2006.08.004

Saberi B, Thakur R, Bhuyan DJ, Vuong QV, Chockchaisawasdee S, Golding JB, Scarlett CJ, Stathopoulos CE (2017) Development of edible blend films with good mechanical and barrier properties from pea starch and guar gum. Starch. https://doi.org/10.1002/star.201600227

Sapper M, Chiralt A (2018) Starch-based coatings for preservation of fruits and vegetables. Rev Coatings 8:152. https://doi.org/10.3390/coatings8050152

Satyamaiah G, Prasad M, Chandrasekhar M, Suhasini DM, Suryanaraya C, Subha MCS, Chowdoji Rao K (2014) Miscibility studies on Guar gum/Pectin blends. Indian J Adv Chem Sci 2(2):116–123

Shehata MG, Darwish AMG, El-Sohaimy SA (2020) Physicochemical, structural and functional properties of water-soluble polysaccharides extracted from Egyptian agricultural by-products. Ann Agricult Sci 65:21–27

Suriyatem R, Auras RA, Rachtanapun P (2019) Utilization of carboxymethyl cellulose from durian rind agricultural waste to improve physical properties and stability of rice starch-based film. J Polym Environ 27:286–298. https://doi.org/10.1007/s10924-018-1343-z

Thakur R, Saberi B, Pristijono P, Stathopoulos CE, Golding JB, Scarlett CJ, Bowyer M, Vuong QV (2017) Use of response surface methodology (RSM) to optimize pea starch–chitosan novel edible film formulation. J Food Sci Technol 54(8):2270–2278. https://doi.org/10.1007/s13197-017-2664-y

Thakur R, Pristijono P, Scarlett CJ, Bowyer M, Singh SP, Vuong QV (2019) Review: Starch-based films: Major factors affecting their properties. Int J Biol Macromol 132:1079–1089. https://doi.org/10.1016/j.ijbiomac.2019.03.1900141-8130

Von Borries-Medrano E, Jaime-Fonseca MR, Aguilar-Méndez MA (2019) Tapioca starch-galactomannan systems: comparative studies of rheological and textural properties. Int J Biol Macromol 122:1173–1183. https://doi.org/10.1016/j.ijbiomac.2018.09.067

Wang L, Xie B, Shi J, Xue S, Deng Q, Wei Y, Tian B (2010) Physicochemical properties and structure of starches from Chinese rice cultivars. Food Hydrocolloids 24:208–216. https://doi.org/10.1016/j.foodhyd.2009.09.007

Zhai Y, Xing J, Luo X, Zhang H, Yang K, Shao X, Chen K, Li Y (2021) Effects of pectin on the physicochemical properties and freeze-thaw stability of waxy rice starch. Foods 10:2419. https://doi.org/10.3390/foods10102419